4-Oxo-2,3,5,6-tetrafluorocyclohexa-2,5-dienylidene—A Highly Electrophilic Triplet Carbene

Wolfram Sander,*[a] Rolf Hübert,[a] Elfi Kraka,[b] Jürgen Gräfenstein,[b] and Dieter Cremer[b]

Dedicated to Wolfgang Kirmse on the occasion of his 70th birthday

Abstract: The 4-oxocyclohexa-2,5-dienylidenes are an interesting class of highly electrophilic carbenes. We investigated the reactivity of the 2,3,5,6-tetrafluorinated and -tetrachlorinated derivatives **1b** and **1c** with small molecules under conditions of matrix isolation. The reactions with molecular oxygen and with carbon monoxide produce the expected carbonyl *O*-oxides and ketenes, respectively. As a result of the extreme electrophilicity of **1b** and **c** both carbenes insert with no or very small activation barriers into H_2 or the CH bonds of hydrocarbons. Obviously, spin restrictions for these formally spin-forbidden reactions do not result in substantial thermal activation barriers.

Keywords: carbenes · electrophiles · insertions · matrix isolation · methane

Introduction

Over the last few years nucleophilic carbenes of the Wanzlick[1, 2] and Arduengo[3, 4] types have found numerous applications in chemistry. However, highly electrophilic carbenes are much less well studied. A major difference between highly nucleophilic and highly electrophilic carbenes is that the former are stable compounds of low reactivity while the latter are extremely reactive even towards most solvents. Thus, difluorovinylidene, an example of an extreme electrophilic singlet carbene, inserts into CH bonds and even into the H_2 molecule with virtually no activation barrier.[5] A group of electrophilic triplet carbenes that have been investigated in our laboratory comprises 4-oxocyclohexadienylidene **1a** and its derivatives, which are easily obtained by photolysis of the corresponding quinone diazides **2** (Scheme 1).[6–10] In matrices, these carbenes exhibit the expected triplet reactivity, for example they react in a diffusion-controlled process with molecular oxygen.[11] An interesting aspect of the photochemistry of carbene **1a** is its reversible rearrangement to the thermodynamically less stable bicyclic isomer **1′a**.[7, 8a, 12]

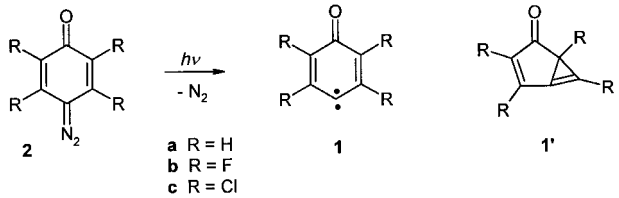

Scheme 1. Photolysis of quinone diazides **2** to yield electrophilic triplet carbenes **1**.

The substitution of the hydrogen atoms in **1a** by the electronegative halogens chlorine and, in particular, fluorine is expected to increase the electrophilicity even further. Studies of the effect of fluorine substitution on the properties of carbenes and nitrenes using direct spectroscopic methods have been described by several authors.[13, 14]

Here we describe the matrix isolation and spectroscopic characterization of the halogenated derivatives 4-oxo-2,3,5,6-tetrafluorocyclohexa-2,5-dienylidene **1b** and 4-oxo-2,3,5,6-tetrachlorocyclohexa-2,5-dienylidene **1c** as examples of highly electrophilic triplet carbenes.

Results and Discussion

Matrix isolation and characterization of carbenes 1b and 1c: The fluorinated quinone diazide **2b** absorbs very strongly in

[a] W. Sander, R. Hübert
Lehrstuhl für Organische Chemie II der Ruhr-Universität
44780 Bochum (Germany)
Fax: (+49) 234-321-4353
E-mail: sander@xenon.orch.ruhr-uni-bochum.de

[b] E. Kraka, J. Gräfenstein, D. Cremer
Theoretical Chemistry, University of Göteborg
Reutersgatan 2, 41320 Göteborg (Sweden)
Fax: (+46) 31-773-5590
E-mail: cremer@theoc.gu.se

  0947-6539/00/0624-4567 $ 17.50+.50/0

the IR at 2108 cm^{-1} (ν_{N-N}) and 1325 cm^{-1} (ν_{C-F}). The calculation of IR spectra is an important tool for the characterization of matrix-isolated compounds, for which, because of cost-efficiency considerations, density functional theory (DFT)[15–20] is often chosen as an appropriate quantum-chemical method. To evaluate the reliability of DFT calculations in reproducing the IR spectra of the fluorinated compounds investigated in this study, we calculated the IR spectrum of **2b** with the standard BLYP[21, 22] and B3LYP functionals[23, 24] and the 6-31G(d) basis set[25] (Figure 1, Table 1). Both methods perform well and nicely reproduce band positions and intensities of the matrix IR spectrum of **2b**. The major difference is that the B3LYP frequencies are systematically too high by ca. 3%; however, if an appropriate scaling procedure is used, the deviations of the calculated from the experimental frequencies are similar. For the chlorinated quinone diazide **2c** a similar agreement between experiment and theory was observed (Figure 2, Table 2). The NN stretching vibration is slightly blue-shifted compared with that of **2b** and found at 2093 cm^{-1}. The CCl stretching vibrations in **2c** are of lower intensity and less characteristic than the corresponding CF stretching vibrations in **2b**.

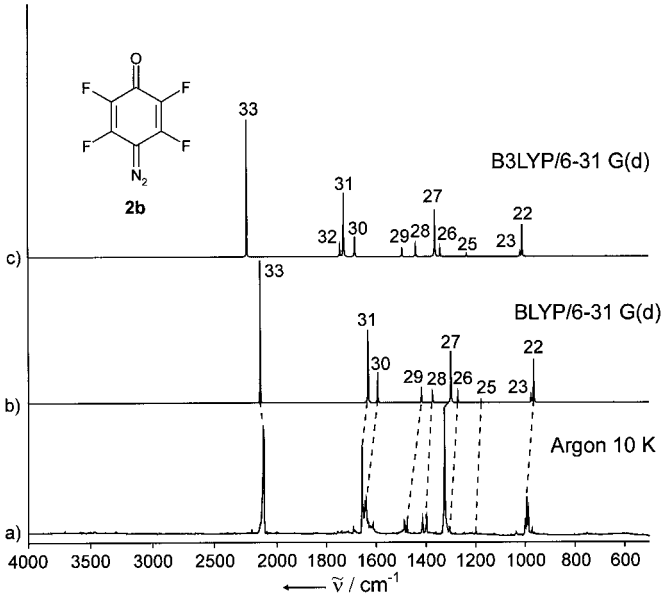

Figure 1. IR spectrum of quinone diazide **2b**. a) Experimental spectrum in argon at 10 K. b) Spectrum calculated at the BLYP/6-31G(d) level of theory. c) Spectrum calculated at the B3LYP/6-31G(d) level of theory.

Table 1. Experimental and calculated IR spectroscopic data of 4-diazo-2,3,5,6-tetrafluorocyclohexa-2,5-diene-1-one (**2b**).

Ar, 10 K		RBLYP/6-31G(d)			RB3LYP/6-31G(d)				
$\tilde{\nu}$ [cm^{-1}]	I[a]	No.[b]	$\tilde{\nu}$ [cm^{-1}]	I[a]	No.[b]	$\tilde{\nu}$ [cm^{-1}]	I[a]	Sym.	Assignment
2108	43	33	2131	100	33	2236	100	A_1	νN=N
1693	3	32	1649	0	32	1744	7	A_1	νC=C
1657	29	31	1632	51	31	1723	47	A_1	νC=O
1641	18	30	1593	21	30	1684	15	B_2	νC=C
1487[c]	8	29	1417	8	29	1493	7	B_2	δC−C
1477[c]	6								
1415[c]	9	28	1372	5	28	1440	8	A_1	δC−C
1399[c]	12								
1325	100	27	1300	36	27	1362	34	A_1	νC−F
1275	1	26	1271	7	26	1341	5	B_2	$\delta_{i.p.}$C−C
1201	3	25	1178	2	25	1235	2	A_1	νC−C
1063	1	24	1097	0	24	1153	0	B_2	νC−F
1002[c]	8	23	978	5	23	1020	3	A_1	$\delta_{i.p.}$C−F
995[c]	21								
990	16	22	966	31	22	1011	23	B_2	$\delta_{i.p.}$C−F
754	2	21	775	0	21	807	0	B_2	$\delta_{i.p.}$C=N
		20	644	0	20	675	0	B_1	τC=O
		19	579	0	19	602	0	A_1	τC=C
		18	527	0	18	560	0	A_2	τC=C
		17	502	0	17	522	0	A_1	$\delta_{i.p.}$ring
		16	462	0	16	491	0	B_1	$\delta_{i.p.}$N=N
		15	455	0	15	484	0	B_2	τC=C
		14	395	0	14	446	0	B_1	$\delta_{i.p.}$N=N
		13	395	1	12	408	1	B_2	$\delta_{i.p.}$C−C
		12	390	0	13	413	0	A_1	τN=N
		11	326	0	11	344	0	A_2	τC−F
		10	323	0	10	340	0	B_1	$\delta_{o.o.p.}$ring
		9	304	1	9	318	1	B_2	$\delta_{i.p.}$C−F
		8	290	0	8	301	0	A_1	$\delta_{i.p.}$C−F
		7	269	0	7	280	0	B_2	$\delta_{i.p.}$C−F
		6	251	0	6	260	0	A_1	$\delta_{i.p.}$C−F
		5	173	1	5	180	1	B_1	$\delta_{o.o.p.}$ring
		4	129	0	4	134	0	B_2	$\delta_{i.p.}$N=N
		3	120	0	3	127	0	A_2	ωC−F
		2	118	0	2	121	0	B_1	ωC=O
		1	65	0	1	66	0	B_1	ωring

[a] Relative intensity based on the most intense absorption (100%). [b] Number of the calculated vibrational modes. The assignment of experimental and calculated IR bands is based on comparison of band positions and relative intensities and is only tentative. [c] IR band is split into two components.

0947-6539/00/0624-4568 $ 17.50+.50/0 *Chem. Eur. J.* **2000**, *6*, No. 24

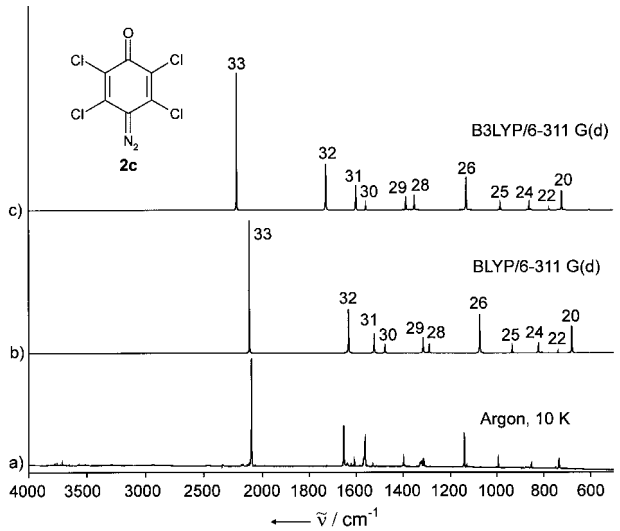

Figure 2. IR spectrum of quinone diazide **2c**. a) Experimental spectrum in argon at 10 K. b) Spectrum calculated at the BLYP/6-311G(d) level of theory. c) Spectrum calculated at the B3LYP/6-311G(d) level of theory.

Visible light irradiation ($\lambda > 515$ nm) of **2b**, matrix-isolated in argon at 10 K, rapidly results in the disappearance of the yellow color of **2b** and appearance of a pale blue color, which is typical of 4-oxocyclohexadienylidenes **1**.[7, 8a] The blue color is caused by a system of very weak absorptions between 680 and 720 nm. In the IR spectrum all IR absorptions of **2b** vanish, and strong absorptions at 1530 cm^{-1} and 1085 cm^{-1}, assigned to carbene **1b** in its triplet ground state (T-**1b**), are formed (Figure 3, Table 3). The assignment of the carbene spectrum is based on comparison with that of other 4-oxocyclohexadienylidenes[8a] and on trapping experiments in the matrix with small molecules. The intense absorption at 1530 cm^{-1} is assigned to the asymmetrical C=C stretching vibration of b_2 symmetry. The corresponding a_1 symmetrical vibration is found at 1582 cm^{-1} and the C=O stretching vibration at 1521 cm^{-1}. The very low frequency of the C=O stretching vibration indicates a CO bond order considerably smaller than two and a π delocalization of one of the unpaired electrons comparable to that of the phenoxy radical.

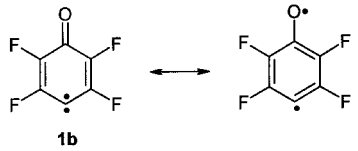

The experimental IR spectrum of **1b** is in agreement with RO-B3LYP calculations of T-**1b**, while there is less agreement

Table 2. Experimental and calculated IR spectroscopic data of 4-diazo-2,3,5,6-tetrachlorocyclohexa-2,5-diene-1-one (**2c**).

Ar, 10 K		RBLYP/6-31G(d)			RB3LYP/6-31G(d)				
$\tilde{\nu}$ [cm^{-1}]	I[a]	No.[b]	$\tilde{\nu}$ [cm^{-1}]	I[a]	No.[b]	$\tilde{\nu}$ [cm^{-1}]	I[a]	Sym.	Assignment
2098[c]	34	33	2113	100	33	2219	100	A_1	νN=N
2093[c]	100								
1654	38	32	1635	37	32	1730	34	A_1	νC=O
1564	24	31	1525	15	31	1602	18	A_1	νC=C
1530	3	30	1478	7	30	1558	4	B_2	νC=C
1399	9	29	1315	12	29	1388	10	B_2	νC–C
1314	7	28	1291	7	28	1351	11	A_1	νC=N
		27	1132	0	27	1205	0	B_2	$\delta_{i.p.}$C=O
1140	28	26	1075	29	26	1131	24	A_1	$\delta_{i.p.}$C=C
995	9	25	936	5	25	986	5	A_1	δC–C
854	3	24	824	8	24	863	5	A_1	$\delta_{i.p.}$C–C
		23	808	1	23	855	1	B_2	νC–Cl
751	2	22	742	1	22	778	1	B_1	τC–C
		21	702	0	21	732	0	B_2	$\delta_{i.p.}$C=N
735	10	20	682	21	20	724	14	B_2	νC–Cl
		19	576	0	19	607	0	B_1	τC–C
		18	542	0	18	573	0	A_2	τC=C
		17	450	0	16	471	0	B_1	νC–Cl
		16	429	0	17	480	0	A_1	τN=N
		15	426	0	15	453	0	B_2	$\delta_{i.p.}$N=N
		14	402	1	14	420	0	A_1	νC–Cl
		13	329	0	13	345	0	B_2	$\delta_{i.p.}$C=O
		12	312	1	12	326	1	A_1	$\delta_{i.p.}$ring
		11	309	0	11	322	0	B_1	$\delta_{o.o.p.}$ring
		10	297	0	10	312	0	A_2	ωC=C
		9	277	0	9	290	0	B_2	$\delta_{i.p.}$ring
		8	207	0	8	216	0	B_2	$\delta_{i.p.}$C–Cl
		7	196	0	7	204	0	A_1	$\delta_{i.p.}$C–Cl
		6	194	0	6	201	0	A_1	$\delta_{i.p.}$C–Cl
		5	148	0	5	155	0	B_1	$\delta_{o.o.p.}$ring
		4	144	0	4	150	0	B_2	$\delta_{i.p.}$N=N
		3	86	0	3	89	0	B_1	$\delta_{o.o.p.}$ring
		2	67	0	2	71	0	A_2	τC–Cl
		1	51	0	1	53	0	B_1	ωring

[a] Relative intensity based on the most intense absorption (100 %). [b] Number of the calculated vibrational modes. The assignment of experimental and calculated IR bands is based on comparison of band positions and relative intensities and is only tentative. [c] IR band is split into two components.

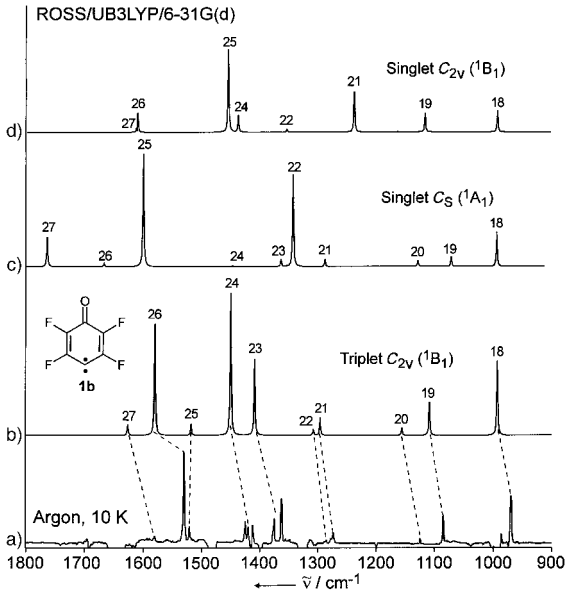

Figure 3. IR spectrum of 4-oxo-2,3,5,6-tetrafluorocyclohexa-2,5-dienylidene (**1b**). a) Experimental spectrum in argon at 10 K. b) Calculated spectrum of the C_{2v}-symmetrical triplet $^3B_1$. c) Calculated spectrum of the C_S-symmetrical closed-shell singlet $^1A_1$. d) Calculated spectrum of the C_{2v}-symmetrical open-shell singlet $^1B_1$.

with both the calculated spectra of the C_S-symmetrical closed-shell singlet state and the C_{2v}-symmetrical open-shell singlet state (Figure 3, Table 3).

Calculations with restricted open-shell DFT (RODFT) for the $^3B_1$ states of **1a** and **1b**, restricted DFT (RDFT) for the corresponding $^1A_1$ ($^1A'$) states, and restricted open-shell singlet DFT (ROSS-DFT)[26, 27] for the corresponding $^1B_1$ states employing the B3LYP hybrid functional reveal that, in contrast to other carbenes, the open-shell singlet state of **1a** is below the closed-shell singlet state, the former being 7, the latter 12 kcal mol^{-1} above the triplet ground state (Table 4). This is in line with other quantum-chemical investigations carried out at the CASSCF(8,8) and CISD + Q levels of theory with a 6-31G(d) basis (CASSCF: 14.5 and 22.7 kcal mol^{-1}; CISD + Q: 10.9 and 17.5 kcal mol^{-1}[28]) although the DFT energy differences are considerably smaller. This indicates the importance of dynamic electron correlation lacking in the CASSCF description and only covered with regard to pair correlation effects at the CISD level, while DFT also includes effects higher than pair correlation, although in an unspecified way. Considering also that in the present work a larger basis (6-311 + G(3df,3pd)[29] as compared to 6-31G(d)) and more reliable geometries (CISD energies were based on CASSCF geometries where CASSCF was unable to find the C_s-symmetrical $^1A'$ state of the closed-shell S)[28] were used, the DFT energy differences of Table 4 are probably more reliable than previous ab initio results. This is confirmed by the fact that Bucher and Sander[8a, 9] predicted an S–T splitting of about 6 kcal mol^{-1} by methanol quenching experiments in a laser-flash photolysis investigation. This value agrees well with the $^3B_1$–$^1B_1$ splitting of 7.0 kcal mol^{-1} calculated in this work.

Since both the $^3B_1$ ground state and the $^1B_1$ open-shell singlet state benefit from delocalization of the pπ single electron at the carbene C into the adjoint π system of the ring,

Table 3. Experimental and calculated IR spectroscopic data of 4-oxo-2,3,5,6-tetrafluorocyclohexa-2,5-dienylidene (**1b**).

Ar, 10 K		$^3B_1$, C_{2v} (ROB3LYP)				$^1A'$, C_S (RB3LYP)				$^1B_1$, C_{2v} (ROSS-B3LYP)				
ν [cm^{-1}]	I_{rel}[a]	No.[b]	ν [cm^{-1}]	I_{rel}[a]	Sym.	No.[b]	ν [cm^{-1}]	I_{rel}[a]	Sym.	No.[b]	ν [cm^{-1}]	I_{rel}[a]	Sym.	Assignment
1581	5	27	1626	7	A_1	27	1754	26	A′	27	1612	1	A_1	νC=C
1530	100	26	1580	78	B_2	26	1657	3	A′	26	1611	23	B_2	νC–C
1521	17	25	1518	8	A_1	25	1590	100	A″	25	1456	100	A_1	νC=O
1425	23	24	1450	100	B_2	24	1436	1	A″	24	1438	20	B_2	νC=C
1420	17	23	1410	54	A_1	23	1353	7	A″	23	1397	0	A_1	$\delta_{i.p.}$C–C
1412	19	22	1308	4	A_1	22	1332	81	A′	22	1354	4	A_1	νC–F
1375	26	21	1296	13	B_2	21	1277	6	A′	21	1239	49	B_2	νC–C
1363	48	20	1156	5	B_2	20	1117	6	A″	20	1163	0	B_2	νC–F
1274	13	19	1109	23	A_1	19	1060	9	A′	19	1116	23	A_1	δC–C
1125	6	18	993	52	B_2	18	983	30	A″	18	992	26	B_2	νC–F
1085	31	17	726	0	B_2	17	735	0	A″	17	724	0	B_2	$\delta_{i.p.}$C–F
986	10	16	701	1	A_1	16	734	1	A′	16	701	0	A_1	δC–C
969	53	15	666	1	B_1	15	676	0	A′	15	662	0	B_1	τC–C
695	5	14	593	1	A_1	14	597	0	A″	14	595	0	A_1	δC–C
586	2	13	588	0	A_2	13	586	0	A′	13	594	0	A_2	τC=C
		12	550	0	B_1	12	571	4	A′	12	559	0	B_1	τC–C
413	2	11	457	0	A_1	11	447	0	A′	11	467	0	A_1	$\delta_{i.p.}$C–C
407	2	10	406	2	B_2	10	444	0	A″	10	416	1	B_2	$\delta_{i.p.}$C–F
		9	368	1	B_1	9	360	1	A″	9	363	0	A_2	τC–C
		8	318	1	A_1	8	353	4	A′	8	358	1	A_1	$\delta_{i.p.}$C–F
		7	309	0	A_1	7	294	2	A′	7	322	0	A_1	$\delta_{i.p.}$C–F
		6	307	0	B_2	6	283	0	A″	6	308	0	B_2	$\delta_{i.p.}$C=O
		5	279	0	B_2	5	252	2	A′	5	281	0	B_2	$\delta_{i.p.}$C–F
		4	259	0	A_1	4	227	1	A″	4	261	0	A_1	ωC=C
		3	195	2	B_1	3	197	1	A′	3	198	1	B_1	δring
		2	127	0	B_1	2	107	0	A′	2	138	0	B_1	ωC=O
		1	118	0	A_2	1	84	0	A″	1	122	0	A_2	ωC–F

[a] All calculations with the 6-31G(d,p) basis set. Relative intensity based on the most intense absorption (100 %). [b] Number of the calculated vibrational modes. The assignment of experimental and calculated IR bands is based on comparison of band positions and relative intensities and is only tentative.

0947-6539/00/0624-4570 $ 17.50+.50/0 *Chem. Eur. J.* **2000**, *6*, No. 24

Table 4. Energies E, relative energies ΔE, enthalpies $H(298)$, relative enthalpies $\Delta H(298)$, dipole moments μ, and number of imaginary frequencies $\#I$ for 4-oxo-cyclohexa-2,5-dienylidene (**1a**) and 4-oxo-2,3,5,6-tetrafluorocyclohexa-2,5-dienylidene (**1b**).[a]

Molecule	State	Sym.	Method[b]	E, ΔE	H, $\Delta H(298)$	μ	$\#I$
Basis: 6-31G(d,p)							
1a	$^3B_1$	C_{2v}	RO	−306.14325	−306.05809	2.97	0
	$^1A'$	C_s	R	13.5	13.2	2.81	0
	$^1A_1$	C_{2v}	R	28.5	27.8	0.70	1
	$^1B_1$	C_{2v}	ROSS	7.0	7.0	2.72	0
1b	$^3B_1$	C_{2v}	RO	−703.03477	−702.97850	2.50	0
	$^1A'$	C_s	R	5.4	5.7	0.56	0
	$^1A_1$	C_{2v}	R	7.8	7.3	1.23	1
	$^1B_1$	C_{2v}	ROSS	6.8	6.8	2.32	0
1′b		C_1	R	12.2	12.8	2.35	0
Basis: 6-311+G(3df,3pd)							
1a	$^3B_1$	C_{2v}	RO	−306.24320	−306.15806	3.21	0
	$^1A'$	C_s	R	12.2	11.9	3.06	0
	$^1A_1$	C_{2v}	R	26.6	25.9	0.84	1
	$^1B_1$	C_{2v}	ROSS	7.2	7.1	2.96	0
1b	$^3B_1$	C_{2v}	RO	−703.30632	−703.25005	2.67	0
	$^1A'$	C_s	R	3.9	4.2	0.62	0
	$^1A_1$	C_{2v}	R	5.6	5.1	1.33	1
	$^1B_1$	C_{2v}	ROSS	7.4	7.4	2.49	0
1′b		C_1	R	11.0	11.6	2.42	0

[a] Energies and enthalpies in Hartree, relative energies and enthalpies in kcal mol^{-1}, dipole moments in Debye. In case of the 6-311+G(3df,3pd) calculations, zero-point energies and thermal corrections were taken from the 6-31G(d,p) results. [b] RO: ROB3LYP; R: RB3LYP; ROSS: ROSS-B3LYP.

these states are close in energy where the T state possesses the lower Coulomb repulsion between the carbene electrons and accordingly becomes the ground state. The degree of π delocalization in these states is directly reflected by the dipole moments (3.2 and 3.0 Debye, Table 4), which indicate that the π system is polarized from the carbene C to the C=O group. The C=C (C–C) bonds in the ring are longer (shorter) than in a suitable reference system where π delocalization is no longer possible, as in the planar $^1A_1$ state of the closed-shell singlet. Polarization of the C=O group leads now to an unstable 4π system that avoids delocalization and suffers in addition from 4-electron repulsion involving the electron lone pair at the carbene C and the bond electron pairs of the neighboring CH bonds. Its dipole moment is just 0.8 Debye because the lone pair distribution at the carbene atom leads to a local dipole moment opposite to that associated with the C=O group. Molecule **1a** can stabilize itself by puckering, thus yielding the C_s-symmetrical $^1A'$ state, which is 14 kcal mol^{-1} more stable than the planar form (transition state for ring inversion), but still 12 and 5 kcal mol^{-1} less stable than the $^3B_1$ ground state and the $^1B_1$ open-shell singlet state, respectively, since it no longer benefits from π delocalization.

Fluorine substitution, as in carbene **1b**, does not change the relative energies of $^3B_1$ ground and $^1B_1$ excited state (Table 4). However, the closed-shell singlet state is strongly stabilized (planar form: 7.8 kcal mol^{-1}, Table 4) so that the C_s-symmetrical $^1A'$ state becomes lower in energy than the $^1B_1$ state, being just 4 kcal mol^{-1} higher than the triplet ground state. This seems to be the result of decreased four-electron repulsion: The σ(C–F) orbital is lower in energy than the σ(C–H) orbital and, therefore, the difference σ(C, lone pair) – σ(C–X) becomes larger, thus decreasing four-electron repulsion. At the same time, there is the possibility of anomeric delocalization of the electron lone pair at the carbene into the σ*(C–F) orbital, which is reflected by an increase in the CF bond length relative to the length of the CF bond vicinal to the keto group (Figure 4). In line with this is the observation that ring folding is reduced from 34.3 (**1a**) to 20.8° (**1b**).

In Table 4 and Figure 4, the relative energy and geometry of the bicyclic isomer **1′b** are also given. For the parent compound the metastable bicyclic isomer **1′a** is about 19 kcal mol^{-1} less stable than the triplet state of **1a**.[28, 30] The highly strained cyclopropene **1′c** is formed during irradiation with visible light of carbene **1a** and, even at temperatures as low as 10 K, thermally rearranges back to the carbene. Fluorination reduces this energy difference by 7 kcal mol^{-1} to 12 kcal mol^{-1} (Table 4), primarily owing to a fluorination effect on the triplet state of the carbene **1**. Despite the smaller energy gap, the bicyclic isomer **1′b** is not formed during the photolysis of **1b**. Our experiments do not allow us to prove whether **1′b** is not formed at all photochemically or if its lifetime is too short to be observable under the conditions of matrix isolation.

The influence of the F substituents on the stability of **1** can be determined with the help of formal reactions such as those represented in Equations (1)–(3). The B3LYP/6-31G(d,p) reaction energy of reaction (1) for **1a** (X = H) is 40, 36, and 64 kcal mol^{-1} for triplet, closed-shell singlet, and open-shell singlet (Table 5) indicating that both inductive and conjugative effects stabilize **1a** where the conjugative stabilization of the open-shell singlet is exceptionally large. The influence of the F substituents is measured by the energy of reaction (2), which is −7.4, 0.6, and −7.3 kcal mol^{-1} (Table 5) for the three states in question, indicating destabilization for the open-shell states and almost no influence in the closed-shell state. This result is largely confirmed when the reference is changed as in reaction (3).

While the data in Table 5 reflect the thermodynamic stability of carbenes **1**, their kinetic stability, in particular their electrophilic character, is reflected by other quantities

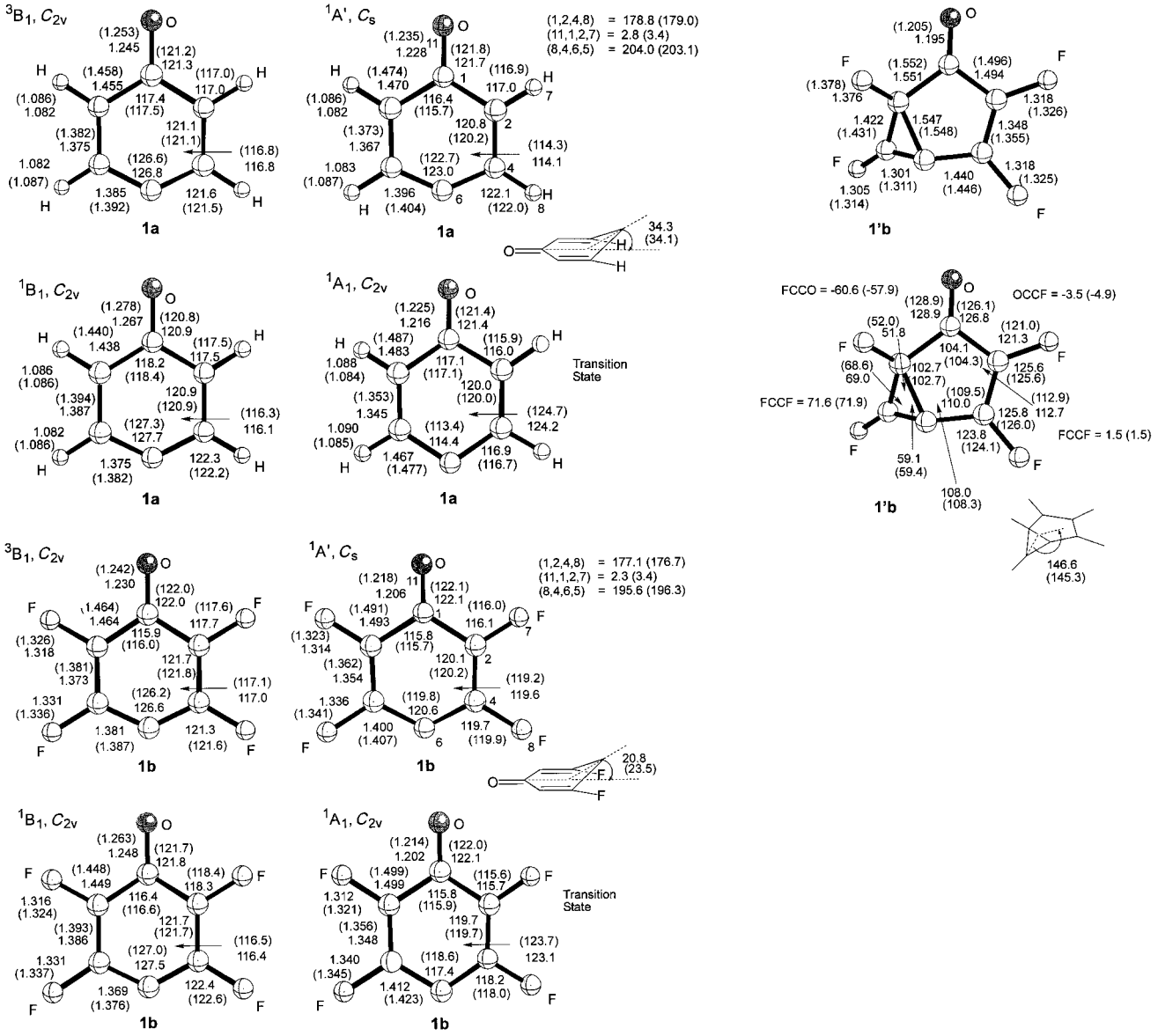

Figure 4. Equilibrium geometries of carbenes **1a**, **1b**, and the bicyclic compound **1'a** calculated at different levels of Kohn–Sham theory employing the 6-311 + G(3df,3pd) basis set (numbers in parentheses refer to geometries obtained with the 6-31G(d,p) basis set). Bond lengths in Å, angles in °. Closed-shell singlet states: RB3LYP; triplet states: ROB3LYP; open-shell singlet states: ROSS-B3LYP.

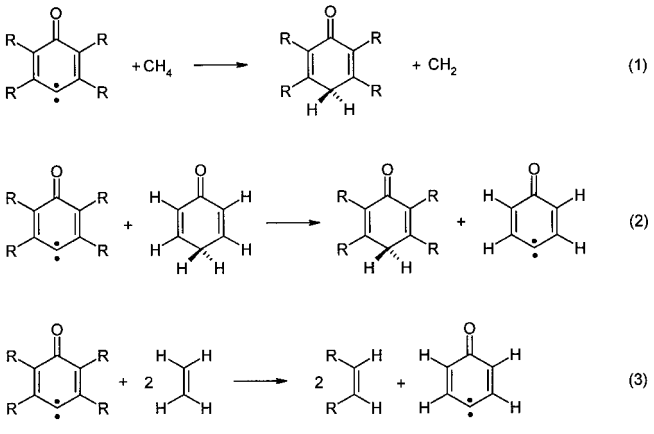

such as the energies of the frontier orbitals and closely related to this the Laplace concentration at the carbene C or the

Table 5. Reaction energies $\Delta_R E$ in kcal mol^{-1} for the formal reactions (1), (2), and (3).

State:	$^3B_1$	$^1A'$	$^1B_1$	
Reaction (1)	X = H	40.0	35.9	64.0
	X = F	32.5	36.5	56.7
Reaction (2)	X = F	−7.4	0.6	−7.3
Reaction (3)	X = F	−5.9	2.1	−5.8

electron affinity (EA) of **1** (Figure 5). The LUMO energy of **1a** is greatly lowered compared to that of the parent carbene while that of **1b** is even further lowered (corresponding to a relatively large EA value); this effect is largest in the closed-shell singlet state. In this state, the

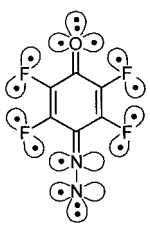

Figure 5. Frontier orbitals of **1**.

0947-6539/00/0624-4572 $ 17.50+.50/0

Laplace concentration has a distinct hole in the π direction at the carbene C characteristic of a strong electrophile that will react with even the weakest donors such as H_2 or CH_4 (see below).

DFT energy data for the loss of N_2 from the quinone diazides **2** show that halogen atoms have a particularly strong influence on the stability of **2** (Table 6). For the parent quinone diazide **2a**, the formation of carbene **1a** is strongly exothermic (B3LYP: −20.6; BLYP: −37.9 kcal mol^{-1}) where

Table 6. DFT reaction energies for the loss of N_2 from quinone diazides **2**.[a]

Reaction	B3LYP/6-31G(d)	BLYP/6-31G(d)
2a → **1a**	−20.6	−37.9
2b → **1b**	+19.6	+19.4
2c → **1c**	−12.4	

[a] All energies in kcal mol^{-1}. For carbene **1**, the triplet state energy calculated at UDFT was used.

spin inversion and the formation of the triplet ground state are assumed in line with experimental observations. Clearly, the exothermicity of the dediazonization of **1a** is dominated by the generation of the stable triple bond in N_2. In contrast, the dediazonization of the fluorinated quinone diazide **2b** is endothermic by almost 20 kcal mol^{-1}, which suggests that fluorination destabilizes **2** by $40 - 7 = 33$ kcal mol^{-1}. Considering that the diazo group strongly increases repulsion between the in-plane lone pairs at F and O, the relatively large destabilization effect becomes understandable. Despite the exothermicity of the reaction of carbene **1b** with molecular nitrogen to give back the diazo compound **2b**, this reaction was not observed in our experiments, indicating that a considerable activation barrier inhibits the formally spin-forbidden reaction.

The tetrachlorocyclohexadienylidene **1c** was synthesized by visible light irradiation ($\lambda > 515$ nm) of quinone diazide **2c**, matrix-isolated in argon at 10 K (Figure 6). The formation of carbene **1c** was indicated by the shift of the color of the matrix

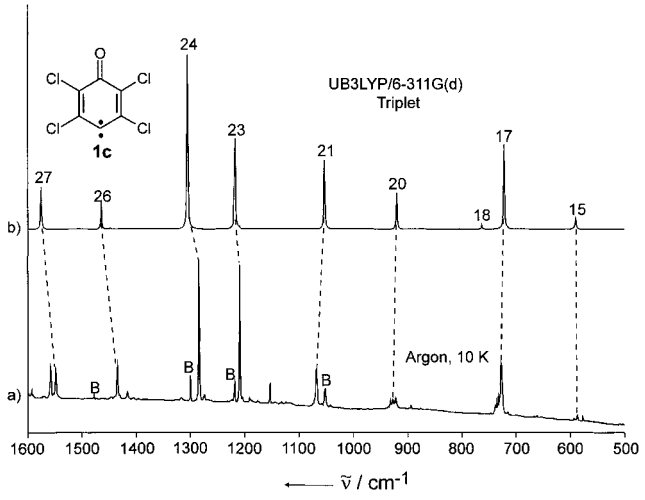

Figure 6. IR spectrum of 4-oxo-2,3,5,6-tetrafluorocyclohexa-2,5-dienylidene (**1b**). a) Experimental spectrum in argon at 10 K. b) Spectrum of the C_{2v} symmetrical triplet $^1B_1$ calculated at the B3LYP/6-311G(d) level of theory.

from yellow to blue, and by the disappearance of all IR absorptions assigned to **2c** and simultaneous appearance of a set of new absorptions (Table 7). Again, the DFT-calculated IR spectrum (UB3LYP/6-311G(d)) is in excellent agreement with the experimental spectrum. The carbonyl stretching vibration is found at 1549 cm^{-1}, slightly blue-shifted compared to that of **1b** (1521 cm^{-1}). The symmetrical and antisymmetrical C=C stretching vibrations are observed at 1411 and 1284 cm^{-1}. The influence of the chlorine substituents on the stability of **2c** is less pronounced. In this case the loss of N_2 is still exothermic, although less than for the parent compound **2a** (Table 6).

Table 7. Experimental and calculated IR spectroscopic data of 4-oxo-2,3,5,6-tetrachlorocyclohexa-2,5-dienylidene (**1c**).

Ar, 10 K		UB3LYP/6-311G(d)				
ν [cm^{-1}]	I[a]	No.[b]	ν [cm^{-1}]	I[a]	Sym.	Assignment
1549	22	27	1575	24	A_1	νC=O
1435	23	26	1464	14	B_2	νC–C
1411	4	25	1447	1	A_1	ν_{sym}C=C
1284	100	24	1306	100	B_2	ν_{asym}C=C
1209	94	23	1217	52	A_1	$\delta_{i.p.}$C–C
1182	3	22	1209	1	B_2	$\delta_{i.p.}$C–C
1068	26	21	1054	40	A_1	$\delta_{i.p.}$C–C
823	7	20	921	21	A_1	$\delta_{i.p.}$C=C
		19	841	0	B_2	$\delta_{i.p.}$C=C
		18	763	3	B_1	τC–C
729	36	17	723	49	B_2	νC–Cl
		16	599	1	A_1	$\delta_{i.p.}$C–C
		15	591	6	B_2	$\delta_{i.p.}$C–C
		14	591	2	B_1	τC–C
		13	573	0	A_2	τC=C
		12	461	2	A_1	$\delta_{i.p.}$C–Cl
		11	343	1	B_2	$\delta_{i.p.}$C–C
		10	336	0	A_1	$\delta_{i.p.}$C–Cl
		9	322	0	B_1	ωC–C
		8	293	0	A_2	ωC=C
		7	274	0	B_2	$\delta_{i.p.}$C=O
		6	202	0	A_1	$\delta_{i.p.}$C–Cl
		5	201	0	B_2	$\delta_{i.p.}$C–Cl
		4	178	0	A_1	$\delta_{i.p.}$C–Cl
		3	146	0	B_1	ωC–C
		2	84	0	B_1	ωC–C
		1	63	0	A_2	ωC–Cl

[a] Relative intensity based on the most intense absorption (100%). [b] Number of the calculated vibrational modes. The assignment of experimental and calculated IR bands is based on comparison of band positions and relative intensities and is only tentative.

Reactions of carbenes 1b and 1c with CO: The trapping of a carbene by CO to give a ketene is highly characteristic and frequently used to identify carbenes.[11] Trapping experiments for the carbenes were carried out in argon matrices doped with 0.5% of CO. Although the concentration of the diazo compounds was not determined, a matrix ratio of >1000:1 is estimated from the experimental conditions of the matrix deposition. The trapping experiments were performed in three steps: i) deposition of the matrix (argon, CO, diazo compound **2** in a ratio of approximately 1000:5:1) at 30 K to obtain optically clear matrices; ii) generation of the carbenes by photolysis of the diazo precursor at 8–10 K; iii) annealing of the matrix at 35–40 K to allow diffusion of small matrix-

isolated molecules (CO) and thus thermal reactions, as long as the activation barriers are small enough ($<1-2$ kcal mol^{-1}).

The IR spectra of the diazo compounds **2b** or **2c** in CO-doped argon show significant blue shifts of the N=N stretching vibration (**2b**: 14; **2c**: 10 cm^{-1}) and red shifts of the C=O stretching (**2b**: -10; **2c**: -5 cm^{-1}), while other vibrations are less affected. This indicates the formation of a complex of the diazo compounds with CO, which results in a higher contribution of the diazonium–phenoxylate resonance structure with a stronger NN and weaker CO bond.

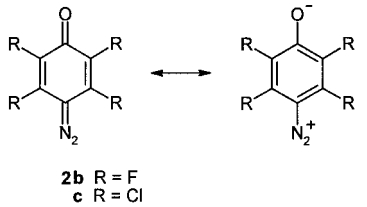

Irradiation of **2b** in argon/CO results in the formation of a product mixture with approximately 30% carbene **1b** and 70% of the ketoketene **4b**. Subsequent annealing at 35 K increases the yield to 85% (Scheme 2). The unusual high yield of trapping product **4b** formed directly after the photolysis of the diazo precursor again suggests the formation of a CO complex during the deposition of the matrix, probably involving the closed-shell singlet state of **1b**.

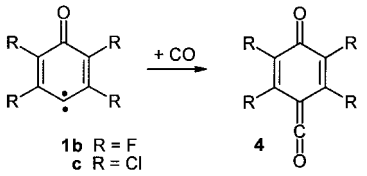

Scheme 2. Carbene **1b**, formed by irradiation of **2b** in argon/CO, is trapped to give ketoketene **4b**.

The IR spectrum of **4b** shows the expected very strong C=C=O stretching vibration at 2172 cm^{-1}. Other characteristic absorptions are the C=O stretching vibration at 1661 cm^{-1}, the asymmetrical C=C stretching vibration at 1653 cm^{-1}, and a C–F stretching vibration at 1323 cm^{-1}. The spectrum was assigned by comparison with that of the known ketene **4a**[7] and by comparison with calculations at the B3LYP/6-31G(d) level of theory.

The trapping of carbene **1c** is completely analogous to that of **1b**. Again a ketoketene with a very strong and characteristic C=C=O stretching vibration at 2132 cm^{-1} is formed. The position of this vibration is halfway between that of **4a** (2110 cm^{-1})[7] and that of **4c** (2173 cm^{-1}), which nicely demonstrates the effect of electron-withdrawing groups in the ring on the ketene group.

Reactions of carbenes 1b and 1c with $^3O_2$: Both triplet and singlet carbenes react with molecular oxygen in its triplet ground state to produce carbonyl *O*-oxides as the primary products,[31] although the formally spin-forbidden reaction of singlet carbenes is much slower.[32] Annealing of a 0.5% O_2-doped argon matrix containing the pale blue carbene **1b** at 35 K rapidly results in the formation of the intensely orange quinone *O*-oxide **5b** (Scheme 3). Comparison of the IR spectrum of **5b** with that of **5a**,[33] ^{18}O isotopic labeling, and

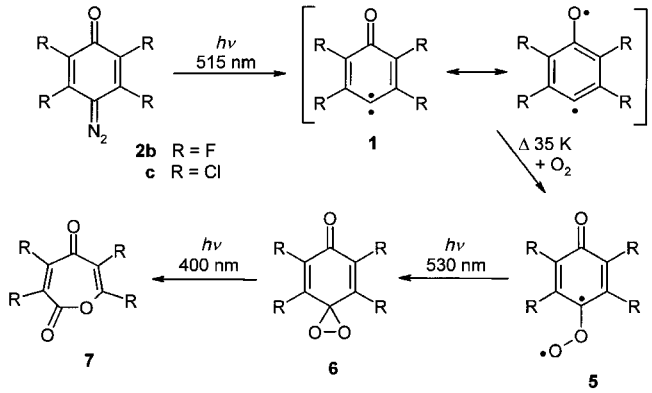

Scheme 3. Reactions of carbenes **1** with triplet oxygen to give carbonyl *O*-oxides and secondary products.

DFT calculations provide the basis for a reliable assignment of the spectrum of **5b** (Figure 7). In the IR spectrum three characteristic vibrations are observed: the C=O stretching vibration at 1627 cm^{-1}, the O–O stretching vibration at 1082 cm^{-1}, and a C–F vibration at 1353 cm^{-1}. The use of

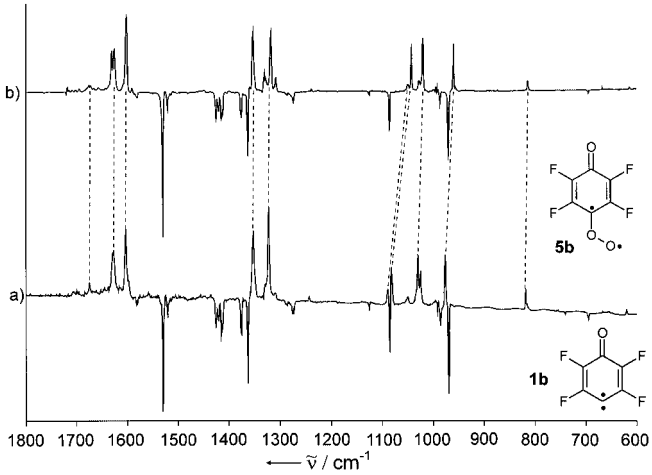

Figure 7. Difference IR spectra showing the thermal reaction of carbene **1b** in an O_2-doped argon matrix at 35 K. Bands pointing downwards are disappearing and assigned to **1b**, bands pointing upwards are appearing and assigned to quinone *O*-oxide **5b**. a) Spectrum obtained with $^{16}O_2$. b) Spectrum obtained with $^{18}O_2$.

$^{18}O_2$ in the reaction with **1b** results in the expected large isotopic shift of the O–O stretching vibration of -40 cm^{-1}. The C=O stretching vibration shows a shift of -26 cm^{-1} while all other vibrations are affected to a much smaller extent. The experimental spectrum is in good accordance with calculations at the BLYP/6-31G(d) level of theory, while B3LYP calculations show larger deviations. The electronic structure of carbonyl oxides can be described as being polar with a substantial degree of biradical character, and therefore only highly correlated ab initio methods succeed in reproducing

0947-6539/00/0624-4574 $ 17.50+.50/0 *Chem. Eur. J.* **2000**, *6*, No. 24

their IR spectra. DFT methods have been shown to perform remarkably well in describing ground-state properties of singlet diradicaloids,[34–36] where in general the B3LYP hybrid functional gives better results, although BLYP may also lead to reasonable results in the case of small basis-set calculations because of fortuitous error cancelations, as was recently shown by Gräfenstein and co-workers.[37]

Carbonyl oxide **5b** is highly photolabile, and irradiation with visible light ($\lambda > 530$ nm) rapidly produces dioxirane **6b**, which on irradiation at 400 nm rearranges to oxepine **7b** (Scheme 3). This sequence is characteristic and frequently used to identify carbenes. Dioxirane **6** and oxepine **7** show the expected characteristic IR absorptions in very good agreement with DFT calculations (B3LYP/6-31G(d)).

The relative energies of the reaction sequence in Scheme 3 were calculated for both the parent (**a**, R = H) and the fluorinated (**b**, R = F) system (Table 8). Although for some of the reaction steps (e.g. **5b** → **6b**) there are differences between the B3LYP and BLYP results, some general trends

Table 8. DFT reaction energies for the oxygenation of carbenes **1** and subsequent rearrangements.[a]

Reaction	B3LYP/6-31G(d)	BLYP/6-31G(d)
1a → **5a**	−50.3	
1b → **5b**	−52.4	−46.2
1c → **5c**	−70.0	
5a → **6a**	−9.7	
5b → **6b**	−16.6	−8.7
5c → **6c**	−17.9	
6a → **7a**	−68.4	
6b → **7b**	−69.7	−68.4
6c → **7c**	−60.0	

[a] All energies in kcal mol^{-1}. For carbene **1**, the triplet state energy calculated at UDFT was used.

for the effect of the fluorination can be extracted. For example, the electronic situations in carbene **1** and carbonyl oxide **5** are comparable, so the fluorination effects in both compounds are similar, a fact reflected by oxygenation energies of −50.3 and −52.4 kcal mol^{-1} for **1a** and **1b**, respectively (Table 6). The formation of dioxirane **6** is an exothermic process, although less than for the parent carbonyl oxide[38] since stereoconjugation in **6** between the a_2-symmetric orbitals of the dioxirane ring (π^*(OO)) and the six-membered ring (π_2) leads to 4-electron destabilizing effects. Since the inductive effects of the F substituents lowers the energy of the π_2 orbital, the 4-electron effects are reduced and the formation of **6b** becomes more exothermic than that of **6a**.

Reaction with hydrogen, methane, and propane: Recently we described the rapid insertion of difluorovinylidene into H_2 under the conditions of matrix isolation.[5b] Difluorovinylidene is a highly electrophilic singlet carbene, and this insertion reaction proceeds without an activation barrier. In this reaction the H–H bond approaches "side-on" at the LUMO of the carbene, and the reaction was estimated to be exothermic by 113.4 kcal mol^{-1} at the B3LYP/6-311G(d,p)+ZPE level of theory. The reaction of carbene **1b** with H_2 to give cyclohexadienone **8b** is also predicted to be highly exothermic by 91.4 kcal mol^{-1} (B3LYP/6-31G(d)), while that of **1c** with H_2, at 73.8 kcal mol^{-1}, is considerably less exothermic (Scheme 4). Since both **1b** and **1c** are triplet ground-state carbenes, the reaction with H_2 to give **8** is formally spin-forbidden and requires an intersystem crossing step along the reaction coordinate. For example, triplet carbene may bind H_2 via the strongly depopulated pπ-orbital at the carbene C, and a spin-flip takes place in combination with an electron jump to the singly filled pσ-orbital.

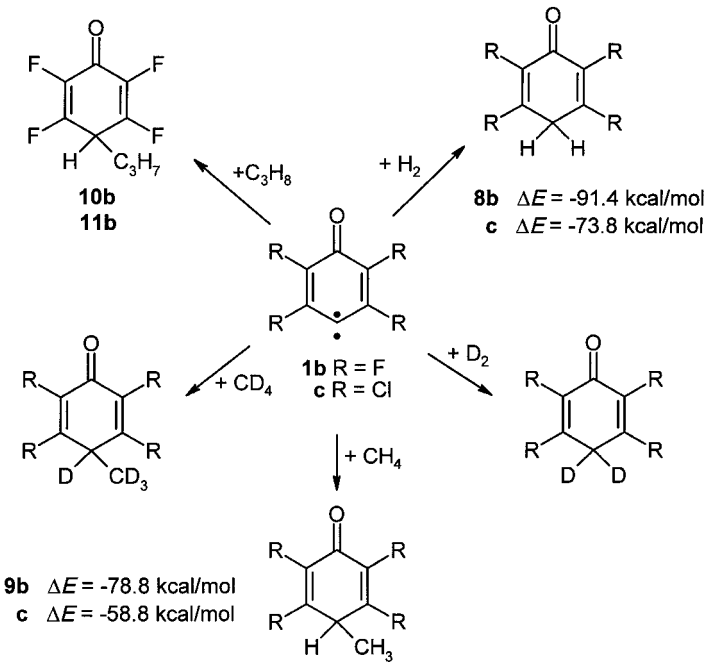

Scheme 4. Reactions of carbenes **1** with hydrogen, methane, and propane.

Irradiation ($\lambda > 515$ nm) of quinone diazide **2b** in matrices produced by deposition of 5% H_2 in argon at 10 K produces carbene **1b** and, in addition, a novel product with several strong absorptions in the carbonyl region of the IR spectrum (Table 9, Figure 8). Because of the high volatility of H_2 even at temperatures as low as 8–10 K the exact concentration of H_2 in the matrix cannot be determined. By comparison with DFT calculations this new compound was assigned the structure of 2,3,5,6-tetrafluorocyclohexa-2,5-dienone **8b** (Scheme 4). The C=O stretching vibration of **8b** is split into two absorptions at 1709 and 1702 cm^{-1}, presumably owing to a Fermi resonance. Similar splittings of the carbonyl absorptions are frequently observed in quinoid compounds. The asymmetrical C=C stretching vibration is found at 1692 cm^{-1}. The assignment of **8b** was confirmed by reacting carbene **1b** with D_2, which produces the deuterated isotopomer [D_2]**8b**. Vibrations with contributions from hydrogen atoms are now easily identified, and the calculated isotopic shifts are in good agreement with experiment.

In typical experiments, irradiation of **2b** in H_2-doped argon matrices at 10 K results in a ratio of **1b**:**8b** of approximately 4:6. Warming of the matrix from 10 K to 35 K further

Table 9. IR spectroscopic data of 2,3,5,6-tetrafluorocyclohexa-2,5-dienone (**8b**) and its deuterated isotopomer [D_2]**8b**, matrix-isolated in argon at 10 K and calculated at the B3LYP/6-31G(d) level of theory.

Ar, 10 K			B3LYP					
ν [cm^{-1}]	I[a]	ν_i/ν[c]	No.[b]	ν [cm^{-1}]	I[a]	ν_i/ν[c]	Sym.	Assignment
			33	3050	0	0.740	B_1	νC–H
			32	3025	1	0.728	A_1	νC–H
			31	1790	0	0.999	A_1	ν_sC=C
1709[d]	95	0.998	30	1772	100	1.000	A_1	νC=O
1702[d]	100	0.997	30	1772	100	1.000	A_1	νC=O
1692	63	0.992	29	1749	58	0.998	B_2	ν_{as}C=C
			28	1481	1	0.955	A_1	$\delta_{i.p.}$C–H
1540	35	0.981	27	1438	21	0.939	B_2	νC–C
1506	15	0.970	26	1372	3	0.980	B_1	νC–C
1309	75	1.000	25	1342	90	1.000	A_2	νC–F
			24	1289	0	0.999	A_1	νC–F
1183	55	0.932	23	1215	38	0.926	B_2	ωC–H
			22	1196	0	0.952	A_1	τC–H
1112	25	0.935	21	1136	11	0.926	B_2	$\delta_{i.p.}$C–F
1101	30	0.840	20	1115	15	0.802	A_2	$\delta_{i.p.}$C–H
			19	967	1	0.923	B_1	$\delta_{i.p.}$C=C
934	50	0.948	18	943	49	0.890	B_1	$\delta_{i.p.}$C–H
929	88	0.865	17	707	4	0.967	A_2	$\delta_{i.p.}$C–C
			16	701	2	0.999	B_2	τC–C
			15	673	0	0.906	B_2	$\delta_{i.p.}$C–C
			14	585	1	0.995	A_2	$\delta_{i.p.}$C–C
			13	560	0	0.971	A_1	τC–C
			12	480	0	0.963	B_1	ωC–C
			11	432	1	0.995	A_1	$\delta_{i.p.}$ring
			10	408	0	0.998	B_2	$\delta_{i.p.}$C–F
			9	344	0	0.977	A_1	ωC=C
			8	317	3	0.997	B_2	$\delta_{i.p.}$C=O
			7	312	1	0.997	A_2	$\delta_{i.p.sym}$C–F
			6	283	0	1.000	B_1	$\delta_{i.p.asym}$
			5	280	0	0.965	B_2	$\delta_{i.p.}$C–H
			4	265	0	0.947	A_1	$\delta_{i.p.sym}$C–F
			3	158	4	0.949	B_1	τC–F
			2	119	0	1.000	A_2	ωC–F
			1	98	0	0.980	B_1	ωC=O

[a] Relative intensity based on the most intense absorption (100%). [b] Number of the calculated vibrational modes. The assignment of experimental and calculated IR bands is based on comparison of band positions and relative intensities and is only tentative. [c] Ratio of vibrational frequencies of the isotopomers [D_2]**8b** and **8b**. [d] Band split into two components.

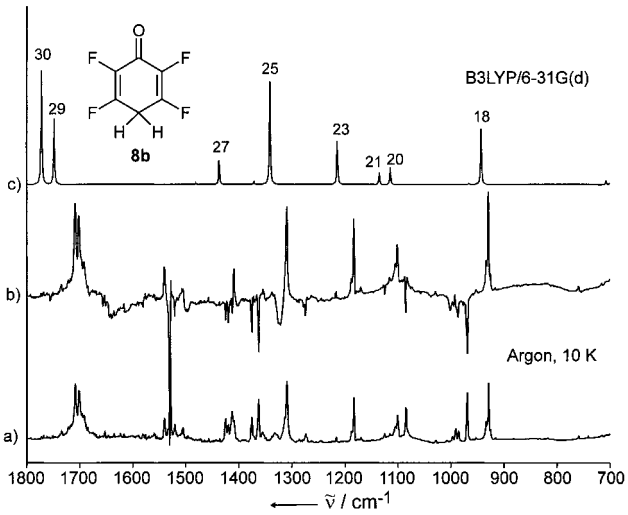

Figure 8. IR spectra showing the thermal reaction of carbene **1b** in an H_2-doped argon matrix at 35 K. a) Spectrum obtained after irradiation of **2b** in H_2/Ar at 10 K, showing a mixture of carbene **2b** and cyclohexadienone **8b**. b) Difference spectrum showing changes on annealing the matrix at 35 K. Bands pointing downwards are disappearing and assigned to **1b**, bands pointing upwards are appearing and assigned to **8b**. c) Spectrum of cyclohexadienone **8b** calculated at the B3LYP/6-31G(d) level of theory.

decreases carbene **1b** and increases the yield of **8b**; this result clearly indicates that the insertion of **1b** into H_2 proceeds with a very small or no activation barrier. This is in line with DFT calculations we carried out for this work, which did not reveal a transition state for the H_2 insertion reaction of **1b**($^1B_1$). With D_2 the same qualitative behavior was observed, a finding that excludes a very large kinetic isotope effect. Our experiments do not allow us to determine at which point of the potential energy surface the intersystem crossing from the triplet to the singlet state occurs. Evidently, the spin restriction does not cause a thermal activation barrier.

Ketone **8b** is the 4*H*-keto tautomer of 2,3,5,6-tetrafluorophenol and is stable under the conditions of matrix isolation. However, at elevated temperatures **8b** is expected to rearrange rapidly by a [1,5]-H migration to the more stable isomeric phenol. The parent cyclohexa-2,5-dienone was trapped at $-196\,^{\circ}C$, but rapidly rearranged to phenol at $-50\,^{\circ}C$.[39]

The chlorinated carbene **1c** also inserts into molecular hydrogen under the conditions of matrix isolation, although the yield of **8c** is somewhat lower than that of **8b**. After irradiation of quinone diazide **2c** in 5% H_2-doped argon matrices at 10 K, 2,3,5,6-tetrachlorocyclohexa-2,5-dienone **8c** is formed in about 40% yield. Again, the insertion product was identified by comparison of experimental and calculated IR spectra. The C=O stretching mode is split into two bands at 1701 and 1694 cm^{-1}, like that of **8b**, and the asymmetrical C=C stretching vibration is found at 1605 cm^{-1}, at considerably lower frequency than that of **8b**.

An important reaction of carbenes is the insertion into C–H bonds, either by hydrogen abstraction followed by radical recombination or by a concerted C–H insertion. The former reaction is expected for triplet and the latter for singlet carbenes. Most carbenes, such as diphenylcarbene as a prototypical triplet and phenylchlorocarbene as a singlet carbene, are completely unreactive towards hydrocarbons under the conditions of matrix isolation.[11] Even the more electrophilic **1a** does not react in a 1% CH_4-doped argon matrix at 40 K. Halogen substituents in **1b** and **1c** increase the electrophilicity of the carbenes, and thus an increase of the reactivity towards C–H bonds is expected. The reaction energy for the insertion of **1b** and **1c** into H_2 is calculated (B3LYP/6-31G(d)) to be -78.8 and -58.8 kcal mol^{-1}, respectively, again showing a smaller exothermicity for the chlorinated compared to the fluorinated carbene.

Irradiation of **2b** in a 1% CH_4-doped argon matrix at 10 K leads to carbene **1b** and approximately 25% of a novel compound with very strong absorptions at 1708 cm^{-1} and 1693 cm^{-1}, which was identified as cyclohexadienone **9b** (Figure 9). Obviously, during the photolysis of **2b** the fraction of methane that is isolated in the same matrix cage directly reacts with carbene **1b** formed during the irradiation. Annealing of the matrix at temperatures between 25 and 40 K results in a further increase of the amount of **9b** which clearly

0947-6539/00/0624-4576 $ 17.50+.50/0 *Chem. Eur. J.* **2000**, *6*, No. 24

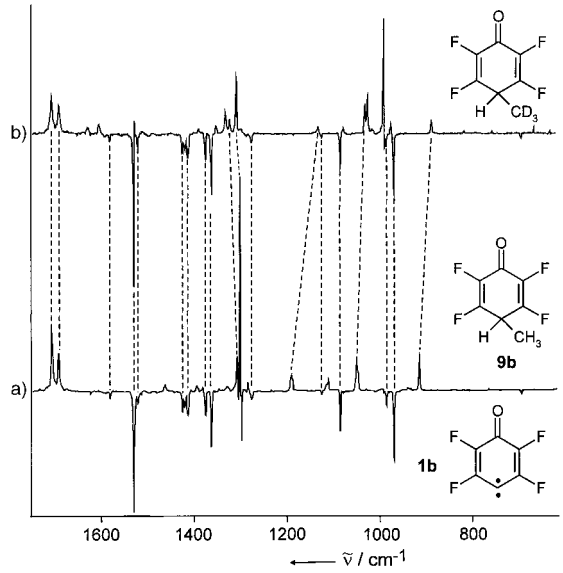

Figure 9. Difference IR spectra showing the thermal reaction of carbene **1b** in CH_4- and CD_4-doped argon matrices at 35 K. Bands pointing downwards are disappearing and assigned to **1b**, bands pointing upwards are appearing and assigned to **9b**. a) Spectrum obtained with CH_4. b) Spectrum obtained with CD_4.

demonstrates that the reaction with methane is a thermal reaction with an extremely small or absent barrier. With CD_4 the corresponding tetradeuterated [D_4]**9b** is formed at qualitatively the same rate, which indicates that the kinetic isotope effect must be small. The IR spectra of **9b** and [D_4]**9b** are in excellent agreement with B3LYP/6-31G(d) calculated spectra. As expected, the deuteration only affects vibrations with a significant contribution of the methyl group.

At room temperature, cyclohexadienylidenes of type **9** are expected to rearrange rapidly by a [1,5]-H migration to the thermodynamically more stable isomeric phenols. However, under the conditions of matrix isolation the tautomerization is not observed.

The reactivity of the tetrachlorinated carbene **1c** towards methane is considerably lower than that of **1b**. Thus, after irradiation of **2c** in 1% CH_4-doped argon matrices, mainly carbene and much lower concentrations of **8c** are formed. After eight hours annealing at 37 K the yield of **8c** is only 34%, while under the same conditions the reaction of **1b** is almost complete.

The reactivity of carbenes **1** in CH_4-doped matrices clearly decreases in the order **1b** > **1c** > **1a**, with **1b** reacting in an approximately diffusion-controlled manner while **1a** does not react at all under the same conditions. This relative order parallels the calculated (B3LYP) exothermicity of the **1** → **8** reaction: −79 kcal mol^{-1} for **1b**, −59 for **1c**, but only −51 kcal mol^{-1} for **1a** (Table 10).

The differences in the reactivities of carbenes **1b** and **1c** are even more pronounced in the reaction with propane, since now only **1b**, but not **1c**, reacts thermally in solid argon. In principle, two insertion products can be formed: insertion into the methyl groups gives **10b**, while insertion into the methylene group produces **11b**. The characteristic and strong IR absorptions of **10b** and **11b** are very similar and the comparison of the experimental spectrum with the spectra calculated for **10b** and **11b** does not permit distinction between these isomers.

Table 10. DFT reaction energies for the insertion of carbenes **1** into hydrogen and methane.[a]

Reaction	B3LYP/6-31G(d)
1b → **8b**	−91.4
1c → **8c**	−73.8
1a → **9a**	−51.2
1b → **9b**	−78.8
1c → **9c**	−58.8

[a] All energies in kcal mol^{-1}. For carbene **1**, the triplet state energy calculated at UDFT was used.

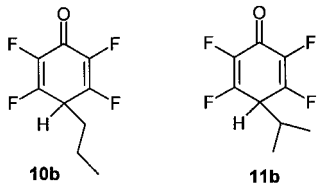

Conclusion

Cyclohexadienylidenes **1** are an interesting class of highly electrophilic triplet ground-state carbenes. Typical reactions, which are also observed for other triplet ground-state carbenes,[11] are the reaction with $^3O_2$ to give carbonyl *O*-oxides **5** and the carbonylation to give ketenes **4**. The introduction of halogen substituents increases the electrophilicity, and **1b** and **1c** are reactive even towards molecular hydrogen and hydrocarbons. Since the "philicity" of carbenes as defined by Moss[40, 41] is difficult to determine for strongly electrophilic carbenes and only defined for singlet ground-state carbenes, the electron affinities EA can be used as a measure of the carbene philicity.[42] In a few cases EAs of carbenes are known experimentally, and it has been shown that EAs can be calculated reliably at the B3LYP level of theory by means of a large basis set (6-311++G(d,p)).[43] EAs of carbenes **1a**–**c** were determined as 2.05, 3.32, and 3.08 eV,[42] indicating a large gap between the halogenated carbenes and **1a**. However, at 2.05 eV the electron affinity of **1a** is still larger than that of (singlet) phenylchlorocarbene (1.52 eV) or (triplet) diphenylcarbene (1.48 eV), a fact that underlines the strongly electrophilic character of oxocyclohexadienylidenes **1**. In summary, the reactivity of carbenes **1** towards H_2 and C–H bonds increases with increasing exothermicity of the insertion reaction as well as with increasing electrophilicity of the carbene.

Experimental Section

General methods and materials: ^{1}H and ^{13}CNMR spectra were recorded in $CDCl_3$ with TMS as internal standard on Bruker AC-200 and AM-400 instruments. IR spectra were obtained with a Bruker IFS66 or Equinox 55 FTIR spectrometer.

Synthesis of diazo precursors

2,3,5,6-Tetrafluoro-1-hydroxy-4-azobenzene: An aqueous solution of sodium nitrite (5.1 g in 26 mL water) was added to a cooled (0 °C) solution of 5.6 g (60 mmol) aniline in 50 mL of hydrochloric acid (6 M) over a period of 30 min. The mixture was added dropwise to a cooled (0 °C) solution of 2,3,5,6-tetrafluorophenol in (10 g in 150 mL 2 M NaOH). After stirring at room temperature for 1 h the mixture was acidified with hydrochloric acid (2 M) to pH 4, which led to the precipitation of a red solid. For further purification the red solid was dissolved in dilute sodium hydroxide (159 mL, 2 M) and filtered. The filtrate was then acidified again to pH 4 with hydrochloric acid (2 M) until the precipitation began. The product was crystallized from glacial acetic acid. Yield: 8.2 g (50 %), m.p.: 178 °C; IR (KBr): $\tilde{\nu}$ (rel. int.) = 3352 (m), 3069 (m), 1685 (w), 1619 (s) 1543 (s), 1509 (vs), 1475 (vs), 1455 (vs), 1350 (s), 1317 (s), 1267 (m), 1226 (s), 1179 (s), 1160 (m), 1111 (m), 1045 (s), 1016 (m), 985 (s), 966 (vs), 881 (m), 773 (m), 755 (m), 691 (m) cm^{-1}; ^1H NMR (200 MHz, CD_3OD): $\delta = 7.54$ (t, 3H), 7.86 (q, 2H); ^1H NMR (200 MHz, $CDCl_3$): $\delta = 3.49$ (s, 1H), 7.51 (t, 3H), 7.90 (d, 2H); ^{13}C NMR (400 MHz, $CDCl_3$): $\delta = 96.53$, 111.40, 133.32, 134.29, 153.29, 196.96; MS (70 eV): m/z (%) = 270 (28) [M^+], 193 (4), 165 (7), 137 (6), 105 (13), 78 (7), 77 (100), 51 (22), 36 (3); elementary analysis: $C_{12}H_6F_4N_2O$ (270): calcd: C 53.35 %, H 2.24 %, N 10.37 %; found: C 51.49 %, H 2.22 %, N 9.85 %.

4-Amino-2,3,5,6-tetrafluorophenol: 8.2 g (30 mmol) of 2,3,5,6-tetrafluoro-1-hydroxy-4-azobenzene were dissolved in 100 mL ethanol and heated to reflux. Under reflux a saturated aqueous solution of sodium dithionite was added until the color changes from deep red to yellow. After heating the mixture to 90 °C for another hour, the ethanol was distilled under vacuum. The black solid obtained was recrystallized from ethanol. Yield: 4.0 g (22 mmol, 73 %), m.p.: 138 °C; IR (KBr): $\tilde{\nu}$ (rel. int.) = 3398 (s), 3306 (s), 2975 (m), 2727 (m), 2649 (m), 1604 (m), 1536 (vs), 1514 (vs), 1463 (m), 1385 (s), 1293 (m), 1206 (s), 1151 (m), 1104 (w), 1007 (s), 954 (vs), 907 (vs), 716 (m), 649 (w), 606 (w) cm^{-1}; MS (70 eV): m/z (%) = 182 (7) [$(M+1)^+$], 181 (100) [M^+], 180 (20) [$(M-1)^+$], 152 (8), 133 (19), 124 (4), 114 (5), 106 (47), 93 (7), 90 (11), 87 (4), 82 (7), 75 (10), 70 (13), 51 (5), 31 (14), 28 (12).

2,3,5,6-Tetrafluoro-1-oxo-4-diazocyclohexa-2,5-dienylidene (1b): Sodium nitrite (0.42 g, 6.1 mmol) was added in small portions (15 min) to a vigorously stirred solution of 4-amino-2,3,5,6-tetrafluorophenol (1 g, 5.5 mmol) and sulfuric acid (70 %, 10 mL) at 0 °C. After the addition of the sodium nitrite the mixture was stirred for two hours at 0 °C. The reaction mixture was poured onto ice (20 g) and extracted with dichloromethane. The combined dichloromethane phases were dried over magnesium sulfate, and the solvent was distilled in vacuo. For further purification the obtained orange solid was dissolved in dichloromethane and purified by liquid chromatography (solid phase: basic aluminium oxide, deactivated with methanol; solvent: dichloromethane). The combined dichloromethane phases were distilled in vacuo, dissolved in a little diethyl ether, precipitated at −60 °C, and filtered on a glass suction filter. Yield: 0.27 g (25 %), m.p.: 65 °C (explosive decomp.); IR (KBr): $\tilde{\nu}$ (rel. int.) = 3441 (vw), 2652 (vw), 2199 (m), 2154 (vs), 1678 (s), 1597 (vs), 1500 (s), 1413 (s), 1396 (s), 1300 (vs), 1129 (vw), 982 (s), 802 (vw), 752 (w), 630 (vw) cm^{-1}; IR (film, soln. in DMSO): $\tilde{\nu}$ (rel. int.) = 3459 (m), 2251 (s), 2126 (s), 1677 (m), 1626 (s), 1604 (s), 1503 (w), 1413 (m), 1309 (s), 1058 (vs) [S=O], 821 (vs), 759 (vs) cm^{-1}; MS (70 eV): m/z (%) = 193 (3) [$(M+1)^+$], 192 (48) [M^+], 166 (25), 165 (4), 164 (45), 136 (78), 117 (100), 99 (11), 86 (17), 82 (5), 79 (9), 74 (13), 69 (7), 62 (4), 55 (12), 31 (70), 28 (67) cm^{-1}.

Caution: The diazo compound **1b** is highly sensitive and explodes on pressure or contact with metals.

Computational methods: DFT calculations were carried out at four different levels of Kohn–Sham theory,[15, 16] namely at restricted DFT (RDFT) for describing closed-shell singlet states, at restricted open-shell DFT (RODFT) and unrestricted open-shell DFT (UDFT) for open-shell triplet states, and at restricted open-shell singlet DFT (ROSS-DFT)[26, 27] for open-shell singlet states. In fact, the description of ROSS states requires at least a two-configurational approach. At the ROSS-DFT level, the two-configuration problem of an open-shell singlet biradical is reformulated in such a way that one can essentially remain within the realm of single-configuration theory at the cost of building up a more complicated Fock matrix. Also, a new exchange correlation (XC) functional has to be constructed for the ROSS case.[26, 27] The ROSS-DFT method has proven to be rather reliable when investigating carbenes,[34] but its use requires that for the comparison of open-shell states RODFT rather than UDFT be employed. However, for the comparison of closed-shell singlet states and open-shell triplet states RDFT and UDFT were used since UDFT covers more electron correlation effects and includes spin polarization.[37] In the case of RDFT calculations for carbenes, the internal and external stability of the R solution were investigated with the help of appropriate stability tests.[44]

Both the BLYP XC functional[21, 22] and the B3LYP hybrid functional [23, 24] were applied since both functionals yield reliable values in the case of carbenes where B3LYP gives the better general performance while BLYP performs well for small basis sets due to a fortuitous cancelation of errors.[37] Routine calculations were performed with the standard 6-31G(d) and 6-31G(d,p) basis sets of Pople.[25] The 6-311 + G(3df,3pd) basis set,[29] which is of VTZ + P quality, was used to obtain a reliable description of the different states of the carbenes investigated.

For each molecule and transition state investigated, vibrational frequencies were obtained to verify the nature of the corresponding stationary point, to determine zero-point energies (ZPE), absolute enthalpies $H(298)$, entropies, etc., and to calculate IR spectra. All IR spectra presented in this work are based on unscaled vibrational frequencies. Calculations were performed with the COLOGNE 99[45] and Gaussian 94 program packages.[46]

Matrix spectroscopy: Matrix isolation experiments were performed by standard techniques with an APD CSW-202 Displex closed-cycle helium cryostat. Matrices were produced by deposition of argon (Linde 99.9999 %) at 30 K on top of a CsI (IR) or sapphire (UV/vis) window at a rate of approximately 0.15 mmol min^{-1}. The samples were produced by codeposition of argon with streams of 4-diazo-2,3,5,6-tetrafluorocyclohexa-2,5-diene-1-one (**1b**) or 4-diazo-2,3,5,6-tetrachlorocyclohexa-2,5-diene-1-one (**1c**) generated by sublimation at 40 °C (**1b**) or (in the case of **1c**) at 96 °C. Irradiation was carried out with Osram HBO 500 W mercury high-pressure arc lamps in Oriel housings equipped with quartz optics. IR irradiation from the lamps was absorbed by a 10 cm path of water and by a Schott KG1 filter. For broad-band irradiation Schott cut-off filters were used (50 % transmission at the wavelength specified), and for narrow-band irradiation, interference filters in combination with dichroic mirrors and cut-off filters were used. Infrared spectra were measured by a Bruker IFS66 FTIR or by an Equinox 55 FTIR spectrometer with a standard resolution of 0.5 cm^{-1} in the range 400 – 4000 cm^{-1}. To avoid photolysis by UV light, all spectra were run with a polished Ge filter with 50 % transmission at 5000 cm^{-1}. UV/Vis spectra were recorded on a Hewlett Packard 8452A diode array spectrophotometer with a resolution of 2 nm.

4-Oxo-2,3,5,6-tetrafluorocyclohexa-2,5-dienylidene (1b): Photolysis (λ = 515 nm) of matrix-isolated 4-diazo-2,3,5,6-tetrafluorocyclohexa-2,5-diene-1-one (**2b**) yielded **1b**: IR (Ar, 10 K): $\tilde{\nu}$ = 1581 (5), 1530 (100), 1521 (17), 1425 (23), 1420 (17), 1412 (19), 1375 (26), 1363 (48), 1274 (13), 1125 (6), 1085 (31), 986 (10), 969 (53), 695 (5), 586 (2), 413 (2), 407 (2) cm^{-1} (rel. int.).

4-Oxo-2,3,5,6-tetrachlorcyclohexa-2,5-dienylide (1c): Photolysis (λ = 515 nm) of matrix-isolated 4-diazo-2,3,5,6-tetrachlorocyclohexa-2,5-diene-1-one (**2c**) yielded **1c**: IR (Ar, 10 K): $\tilde{\nu}$ = 1549 (22), 1435 (23), 1411 (4), 1284 (100), 1209 (94), 1182 (3), 1068 (26), 823 (7), 729 (36) cm^{-1} (rel. int.).

2,3,5,6-Tetrafluorocyclohexa-2,5-dienone *O*-oxide (5b): Oxidation (Ar/1 % O_2, 35 K) of matrix-isolated **1b** produced carbonyl oxide **5b**. IR (Ar, 10 K): $\tilde{\nu}$ = 1674 (12), 1627 (47), 1603 (71), 1353 (72), 1322 (100), 1310 (6), 1260 (5), 1089 (16), 1082 (40), 1030 (52), 1025 (359, 976 (53), 819 (19), 590 (59) cm^{-1} (rel. int.).

4,5,7,8-Tetrafluoro-1,2-dioxaspiro[2.5]-4,7-diene-6-one (6b): Photolysis (Ar/1 % O_2, λ = 530 nm) of matrix-isolated **5b** yielded **6b**: IR (Ar, 10 K): $\tilde{\nu}$ = 1730 (3), 1719 (33), 1709 (40), 1695 (50), 1402 (8), 1372 (44), 1333 (100), 1320 (1), 1221 (7), 1125 (1), 1028 (18), 996 (18), 992 (83), 887 (5), 763 (5), 758 (3), 695 (1) cm^{-1} (rel. int.).

2,3,5,6-Tetrachlorocyclohexa-2,5-dienone *O*-oxide (5c): Oxidation (Ar/1 % O_2, 35 K) of matrix-isolated **1c** produced carbonyl oxide **5c**: IR (Ar, 10 K): $\tilde{\nu}$ = 1642 (24), 1585 (5), 1473 (16), 1358 (2), 1322 (3), 1240 (13), 1151 (100), 1097 (3), 998 (23), 887 (3), 856 (3), 754 (10), 750 (20), 640 (2), 509 (2) cm^{-1} (rel. int.).

4,5,7,8-Tetrachloro-1,2-dioxaspiro[2.5]-4,7-diene-6-one (6c): Photolysis (Ar/1 % O_2, λ = 530 nm) of matrix-isolated **5c** yielded **6c**: IR (Ar, 10 K): $\tilde{\nu}$ = 1701 (65), 1623 (3), 1586 (47), 1319 (12), 1278 (2), 1236 (13), 1121 (100), 1114 (39), 1033 (4), 893 (12), 883 (5), 797 (1), 739 (45), 697 (7), 638 (2) cm^{-1} (rel. int.).

0947-6539/00/0624-4578 $ 17.50+.50/0 *Chem. Eur. J.* **2000**, *6*, No. 24

4-Methyl-4′-hydro-2,3,5,6-tetrafluorocyclohexa-2,5-diene-1-one (9b): Reaction (Ar/1% CH_4, 35 K) of matrix-isolated **1b** produced **9b**: IR (Ar, 10 K): $\tilde{\nu}$ = 173 (5), 1708 (100), 1693 (67), 1463 (13), 1437 (3), 1395 (10), 1347 (59, 1307 (61), 1284 (13), 1190 (26), 1111 (21), 1051 (49), 940 (3), 915 (64), 765 (1), 668 (1), 605 (19) cm^{-1} (rel. int.).

4-Methyl-4′-hydro-2,3,5,6-tetrachlorocyclohexa-2,5-diene-1-one (9c): Reaction (Ar/1% CH_4, 35 K) of matrix-isolated **1c** produced **9c**: IR (Ar, 10 K): $\tilde{\nu}$ = 1696 (100), 1619 (20), 1596 (39), 1454 (6), 1265 (20), 1116 (88), 1063 (20), 1001 (25), 878 (6), 838 (4), 726 (31), 638 (2) cm^{-1} (rel. int.).

4-Isopropyl-4′-hydro-2,3,5,6-tetrafluorocyclohexa-2,5-diene-1-one (10b): Reaction (Ar/1% C_3H_8, 35 K) of matrix-isolated **1b** produced **10b**: IR (Ar, 10 K): $\tilde{\nu}$ = 1706 (100), 1686 (56), 1576 (2), 1558 (2), 1401 (18), 1384 (6), 1352 (2), 1316 (42), 1308 (30), 1299 (91), 1253 (3), 1185 (49), 1153 (3), 1104 (22), 1081 (16), 1029 (3), 943 (33), 936 (73), 872 (6), 778 (5), 746 (6), 611 (29) cm^{-1} (rel. int.).

2,3,5,6-Tetrafluorocyclohexa-2,5-dienone (8b): Reaction (Ar/1% H_2, 35 K) of matrix-isolated **1b** produced **8b**: IR (Ar, 10 K): $\tilde{\nu}$ = 1709 (95), 1702 (100), 1692 (63), 1540 (35), 1506 (15), 1309 (75), 1183 (55), 1112 (25), 1101 (30), 934 (50), 929 (88) cm^{-1} (rel. int.).

2,3,5,6-Tetrachlorocyclohexa-2,5-dienone (8c): Reaction (Ar/1% H_2, 35 K) of matrix-isolated **1c** produced **8c**: IR (Ar): $\tilde{\nu}$ = 1701 (69), 1694 (91), 1628 (24), 1605 (69), 1450 (4), 1396 (13), 1255 (24), 1124 (100), 1121 (58), 1098 (18), 1038 (40), 938 (4), 838 (3), 746 (3), 728 (56), 580 (9) cm^{-1} (rel. int.).

2,3,5,6-Tetrafluorocyclohexa-2,5-diene-1-one-4-ketene (4b): Reaction (Ar/0.5% CO, 35 K) of matrix-isolated **1b** produced **4b**: IR (Ar, 10 K): $\tilde{\nu}$ = 2173 (100), 1703 (4), 1661 (32), 1653 (22), 1453 (10), 1417 (8), 1323 (80), 1203 (2), 1118 (2), 998 (10), 991 (9), 980 (26), 809 (2) cm^{-1} (rel. int.).

Acknowledgements

This work was financially supported by the Deutsche Forschungsgemeinschaft and the Fonds der Chemischen Industrie at the University of Bochum while at Göteborg University support was provided by the Swedish Natural Science Research Council (NFR). Calculations were done on the CRAY C90 of the Nationellt Superdatorcentrum (NSC), Linköping (Sweden). The authors thank the NSC for a generous allotment of computer time.

[1] H.-W. Wanzlick, *Angew. Chem.* **1962**, *74*, 129–134; *Angew. Chem. Int. Ed. Engl.* **1962**, *1*, 75–80.
[2] A. J. I. Arduengo, J. R. Goerlich, R. Krafczyk, W. J. Marshall, *Angew. Chem.* **1998**, *110*, 2062–2064; *Angew. Chem. Int. Ed.* **1998**, *37*, 1963–1965.
[3] A. J. I. Arduengo, R. L. Harlow, M. Kline, *J. Am. Chem. Soc.* **1991**, *113*, 361–363.
[4] A. J. I. Arduengo, H. V. R. Dias, R. L. Harlow, M. Kline, *J. Am. Chem. Soc.* **1992**, *114*, 5530–5534.
[5] a) W. Sander, C. Kötting, *Chem. Eur.J.* **1999**, *5*, 24–28; b) C. Kötting, W. Sander, *J. Am. Chem. Soc.* **1999**, *121*, 8891–8897.
[6] W. Sander, G. Bucher, P. Komnick, J. Morawietz, P. Bubenitschek, P. G. Jones, A. Chrapkowski, *Chem. Ber.* **1993**, *126*, 2101–2109.
[7] W. Sander, G. Bucher, F. Reichel, D. Cremer, *J. Am. Chem. Soc.* **1991**, *113*, 5311–5322.
[8] a) G. Bucher, W. Sander, *J. Org. Chem.* **1992**, *57*, 1346–1351; b) G. Bucher, W. Sander, *Chem. Ber.* **1992**, *125*, 1851–1859.
[9] B. R. Arnold, J. C. Scaiano, G. F. Bucher, W. W. Sander, *J. Org. Chem.* **1992**, *57*, 6469–6474.
[10] W. Sander, G. Bucher, H. Wandel, E. Kraka, D. Cremer, W. S. Sheldrick, *J. Am. Chem. Soc.* **1997**, *119*, 10660–10672.
[11] W. Sander, G. Bucher, S. Wierlacher, *Chem. Rev.* **1993**, *93*, 1583–1621.
[12] W. Sander, A. Kirschfeld, *Matrix Isolation of Strained Three-Membered Ring Systems* in *Advances in Strain in Organic Chemistry* (Ed.: B. Halton), JAI, London, **1995**, pp. 1–80.
[13] X. M. Du, H. Fan, J. L. Goodman, M. A. Kesselmayer, K. Krogh-Jespersen, J. A. LaVilla, R. A. Moss, S. Shen, R. S. Sheridan, *J. Am. Chem. Soc.* **1990**, *112*, 1920–1926.
[14] a) A. Admasu, A. D. Gudmundsdottir, M. S. Platz, *J. Phys. Chem. A* **1997**, *101*, 3832–3840; b) M. J. T. Young, M. S. Platz, *J. Org. Chem.* **1991**, *56*, 6403–6406; c) R. Poe, K. Schnapp, M. J. T. Young, J. Grayzar, M. S. Platz, *J. Am. Chem. Soc.* **1992**, *114*, 5054–5067; d) K. A. Schnapp, M. S. Platz, *Bioconjugate Chem.* **1993**, 178–183; e) J. Michalak, H. B. Zhai, M. S. Platz, *J. Phys. Chem.* **1996**, *100*, 14028–14036.
[15] P. Hohenberg, W. Kohn, *Phys. Rev.* **1964**, *136*, B864.
[16] W. Kohn, L. J. Sham, *Phys. Rev.* **1965**, *140*, A1133.
[17] *Modern Density Functional Theory* (Eds.: J. M. Seminario, P. Politzer), Elsevier, Amsterdam, *1995*.
[18] *Chemical Applications of Density-Functional Theory* (Eds.: B. B. Laird, R. B. Ross, T. Ziegler), *ACS Symp. Ser.*, *Vol. 629*, American Chemical Society, Washington DC, **1996**.
[19] *Density Functional Theory I–IV* (Ed.: R. F. Nalewajski), *Top. Curr. Chem.*, *Vol. 180–183*, **1996**.
[20] *Density-Functional Methods in Chemistry and Materials Science* (Ed.: M. Springborg), Wiley, Chichester, **1997**.
[21] A. D. Becke, *Phys. Rev. A: Gen. Phys.* **1988**, *38*, 3098–3100.
[22] C. Lee, W. Yang, R. G. Parr, *Phys. Rev. B: Condens. Matter* **1988**, *37*, 785–789.
[23] A. Becke, *J. Chem. Phys.* **1993**, *98*, 5648–5652.
[24] P. J. Stephens, F. J. Devlin, C. F. Chabalowski, M. J. Frisch, *J. Phys. Chem.* **1993**, *98*, 11623.
[25] P. C. Hariharan, J. A. Pople, *Chem. Phys. Lett.* **1972**, *66*, 217.
[26] J. Gräfenstein, E. Kraka, D. Cremer, *Chem. Phys. Lett.* **1999**, *288*, 593.
[27] W. Sander, H. Wandel, G. Bucher, J. Gräfenstein, E. Kraka, D. Cremer, *J. Am. Chem. Soc.* **1998**, *120*, 8480–8485.
[28] A. Sole, S. Olivella, J. M. Bofill, J. M. Anglada, *J. Phys. Chem.* **1995**, *99*, 5934–5944.
[29] R. Krishnan, M. J. Frisch, J. A. Pople, *J. Chem. Phys.* **1980**, *72*, 4244–4245.
[30] R. Albers, W. Sander, C.-H. Ottosson, D. Cremer, *Chem. Eur. J.* **1996**, *2*, 967–973; R. Albers, W. Sander, C.-H. Ottosson, D. Cremer, *Angew. Chem.* **1996**, *108*, 825–827; *Angew. Chem. Int. Ed. Engl.* **1996**, *35*, 746–748.
[31] W. Sander, *Angew. Chem.* **1990**, *102*, 362–372; *Angew. Chem. Int. Ed. Engl.* **1990**, *29*, 344–354.
[32] G. A. Ganzer, R. S. Sheridan, M. T. H. Liu, *J. Am. Chem. Soc.* **1986**, *108*, 1517–1520.
[33] W. W. Sander, *J. Org. Chem.* **1988**, *53*, 2091–2093.
[34] J. Gräfenstein, D. Cremer, *Phys. Chem. Chem. Phys.* **2000**, *104*, 1748.
[35] E. Kraka, C. P. Sosa, D. Cremer, *Chem. Phys. Lett.* **1996**, *260*, 43–50.
[36] R. Gutbrod, R. N. Schindler, E. Kraka, D. Cremer, *Chem. Phys. Lett.* **1996**, *252*, 221–229.
[37] J. Gräfenstein, A. M. Hjerpe, E. Kraka, D. Cremer, *J. Chem. Phys.* **2000**, *104*, 1748–1761.
[38] D. Cremer, E. Kraka, P. G. Szalay, *Chem. Phys. Lett.* **1998**, *292*, 97–109.
[39] M.-C. Lasne, J.-L. Ripoll, *Tetrahedron Lett.* **1980**, *21*, 463–464.
[40] R. A. Moss, *Acc. Chem. Res.* **1980**, *13*, 58–64.
[41] R. A. Moss, *Acc. Chem. Res.* **1989**, *22*, 15–21.
[42] W. Sander, C. Kötting, R. Hübert, *J. Phys. Org. Chem.* **2000**, *13*, 561–568.
[43] G. S. Tschumper, H. F. Schaefer III, *J. Chem. Phys.* **1997**, *107*, 2529–2541.
[44] R. Bauernschmitt, R. Ahlrichs, *J. Chem. Phys.* **1996**, *104*, 9047–9052.
[45] E. Kraka, J. Gräfenstein, J. Gauss, F. Reichel, L. Olsson, Z. Konkoli, Z. He, D. Cremer, *COLOGNE 99*, Göteborg University, Göteborg, **1999**.
[46] M. J. Frisch, G. W. Trucks, H. B. Schlegel, P. M. W. Gill, B. G. Johnson, M. A. Robb, J. R. Cheeseman, T. Keith, G. A. Petersson, J. A. Montgomery, K. Raghavachari, M. A. Al-Laham, V. G. Zakrzewski, J. V. Ortiz, J. B. Foresman, C. Y. Peng, P. Y. Ayala, W. Chen, M. W. Wong, J. L. Andres, E. S. Replogle, R. Gomperts, R. L. Martin, D. J. Fox, J. S. Binkley, D. J. Defrees, J. Baker, J. P. Stewart, M. Head-Gordon, C. Gonzalez, J. A. Pople, *Gaussian 94*, *Revision B.3*, Gaussian, Pittsburgh PA, **1995**.

Received: April 28, 2000 [F2450]